Bifurcations of indifference points in discrete time optimal control problems

Mohammadian Moghayer, S.

Chapter 4

Numerics of invariant manifolds, indifference points, and indifference-attractor bifurcations

In Chapter 3 the genesis of indifference thresholds in an indifference-attractor bifurcation is studied for a class of non-convex infinite horizon discrete-time optimal control problems. This chapter presents details of the computation of optimisers and bifurcation curves.

As in Chapter 3 a geometrical point of view is taken. Unlike the well-known iterative methods of numerical dynamic programming (see Judd (1998)), the algorithms presented in this chapter are based on the direct computation of stable manifolds. It is usually impossible to determine analytic expressions for these invariant manifolds, so numerical computations are needed.

Details are given of a simple method which accurately computes arbitrarily long segments of an invariant manifold. This information is used to compute the locus of the indifference-attractor bifurcation points of the problem.

The chapter is organised as follows. In Section 4.1 the optimisation problem is recalled and the main results obtained in Chapter 3 are sketched briefly. In Section 4.2 the numerical method for computing stable manifold is given. Based on this in Section 4.3 methods to determine optimal solutions, value functions and thresholds as well as indifference points are given. In Section 4.4 a method to compute indifference-attractor bifurcations is presented.

4.1 The family of optimisation problems

A family of problems of maximising an objective

$$J_\mu(\mathbf{x}, \mathbf{u}) = \sum_{t=1}^{\infty} g(x_{t-1}, u_t; \mu)\, \mathrm{e}^{-\rho t}. \tag{4.1}$$

is considered. The family depends on a system parameter μ. The discount rate ρ is assumed to be positive. The maximisation is performed over all pairs of sequences $\mathbf{x} = \{x_t\}$ and $\mathbf{u} = \{u_t\}$ such that $x_t \in \mathscr{X}$, $u_t \in \mathscr{U}$ and such that for all $t = 1, 2, ...,$

$$x_t = f(x_{t-1}, u_t; \mu). \tag{4.2}$$

The parameter μ takes values in the parameter space $\mathscr{P} \subset \mathbb{R}$, which is an open and bounded interval. Also $\mathscr{X} \subset \mathbb{R}$ and $\mathscr{U} \subset \mathbb{R}$ are open intervals. The initial state x_0 is assumed to be given. The functions f and g are assumed to be smooth, i.e. C^∞, in the interior of $\mathscr{X} \times \mathscr{U}$, and their derivatives are assumed to be bounded there. Moreover, it is assumed that $f(x, u; \mu) \in \mathscr{X}$

for all $(x, u; \mu)$, and that the partial derivative $f_u(x, u; \mu)$ does not vanish anywhere.

Recall definition (2.8) of the costate variable y and of the phase map φ of the problem (see Section 2.1.4). In terms of these, the necessary first order conditions of the problem are formulated as the following boundary value problem: if $(\mathbf{x}, \mathbf{y})$ is maximising and $\delta-$interior, for $\delta > 0$, then

$$(x_t, y_t) = \varphi(x_{t-1}, y_{t-1}),$$
$$x_0 = \alpha \quad \text{and} \quad \lim_{t\to\infty} e^{-\rho t} y_t = 0.$$

Recall moreover that if an optimal state trajectory $\mathbf{x}$ converges to some steady state, this state corresponds to a fixed point of the phase map φ.

The main result of Chapter 3 has been obtained in the following setting. The parametrised family $\varphi = \varphi_\mu$ of phase maps associated to the optimisation problem (4.1) depends smoothly on a parameter $\mu \in \mathscr{P}$. Every map $\varphi = \varphi_\mu$ is assumed to have at least two saddle fixed points $z_\pm = (x_\pm, y_\pm)$, with $x_- < x_+$.

Recall from Chapter 3 that the family φ_μ is said to go through a heteroclinic bifurcation scenario involving W^u_- and W^s_+, if there is a parameter interval $[\mu_1, \mu_2] \subset \mathscr{P}$ such that for $\mu < \mu_1$ and $\mu > \mu_2$, the manifolds W^u_- and W^s_+ have no points in common, while for $\mu \in [\mu_1, \mu_2]$ there is at least one heteroclinic orbit. Recall moreover that all heteroclinic orbits are necessarily tangencies at $\mu = \mu_1$ and $\mu = \mu_2$. Assumptions 3.1–3.5 imply that the family φ_μ of phase maps goes through a heteroclinic bifurcation scenario.

Theorem 3.1.1 states that there is a parameter value $\mu_c \in (\mu_1, \mu_2)$ such that for $\mu < \mu_c$, the steady state x_+ is globally optimal. If $\mu > \mu_c$, both

steady states are locally optimal, and there is a state $x_- < x_s < x_+$ such that x_s is initial state to two optimal solutions of which one converges to x_- and the other converges to x_+. This is summarised by saying that at μ_c the solution structure exhibits an indifference-attractor bifurcation.

4.2 Invariant Manifolds

Optimal solutions correspond to trajectories on one of the stable manifolds. In order to compute these solutions the manifolds need to be approximated numerically. This is achieved by first computing a local stable manifold, and then extending it iteratively.

Consider therefore a saddle fixed point $\bar{z}$ of the map φ. Let E^s and E^u be the stable and unstable eigenspaces of $D\varphi(\bar{z})$ corresponding to λ^s and λ^u respectively. A linear change of coordinates is performed such that $\bar{z}$ corresponds to the origin, E^s to the x-axis and E^u to the y-axis. Then

$$\varphi(z) = \begin{pmatrix} \lambda^s & 0 \\ 0 & \lambda^u \end{pmatrix} \begin{pmatrix} x \\ y \end{pmatrix} + O(|z|^2),$$

where $z = \begin{pmatrix} x \\ y \end{pmatrix}$ and $0 < \lambda^s < 1 < \lambda^u$.

Recall that W^s is a smooth manifold, tangent to E^s at the fixed point. Locally around the origin W^s can therefore be parametrised as $y = w(x)$ with $w(0) = 0$ and $w'(0) = 0$. Moreover, since W^s is invariant under φ, the function w has to satisfy the functional equation

$$w\big(\varphi_1\big(x, w(x)\big)\big) = \varphi_2\big(x, w(x)\big). \tag{4.3}$$

Finding a local stable manifold amounts to solving (4.3) numerically.

4.2.1 Computing the local stable manifold. For the computation of invariant manifolds there are several approaches: a naive approach is to take points on E^s and obtain a discrete approximation of W^s by computing backward iterations of these points. A more sophisticated approach takes the graph transform as its starting point, obtaining the invariant manifold as a fixed point of a discrete graph transform operator. Based on this, Homburg et al. (1995) derived a numerical algorithm for the computation of invariant manifolds of hyperbolic fixed points using invariant foliations. Yet other methods are based on obtaining the coefficients of an expansion $w(x) = \sum a_n x^n$ (cf. Simó (1989)). The approach proposed in this section was suggested by F. Takens; while less sophisticated than the methods referred to, it still provides accurate approximations to the stable manifolds. It is however restricted to two-dimensional systems.

For a given point $(\hat{x}, 0) \in E^s$ the algorithm will determine an approximation $(\hat{x}, \hat{w})$ to $\big(\hat{x}, w(\hat{x})\big) \in W^s$. For $\delta > 0$, define $R = [0, \hat{x}] \times [-\delta, \delta]$. Set $z_0 = (\hat{x}, y_0)$ with $-\delta \leq y_0 \leq \delta$ and consider the orbit $\mathbf{z} = \{z_t\}$ of φ starting at z_0. There are two possibilities: if $y_0 = w(\hat{x})$, then z_t converges towards the origin as $t \to \infty$. In particular this means that $z_t \in R$ for all $t > 0$. If however $y_0 \neq w(\hat{x})$, then the orbit will leave the rectangle R eventually; that is, there is $T > 0$ such that $z_t \in R$ if $0 \leq t < T$ and $z_T \notin R$. Based on the linear approximation $\varphi(x) \approx D\varphi(0)\, x$, the following approximation is obtained

$$T \approx \left[\frac{-\log |y_0 - w(\hat{x})| + \log \delta}{\log \lambda^u} \right].$$

Note moreover that if $y_0 > w(\hat{x})$ then $y_T > \delta$; if $y_0 < w(\hat{x})$ then $y_T < -\delta$. The algorithm is based on this observation.

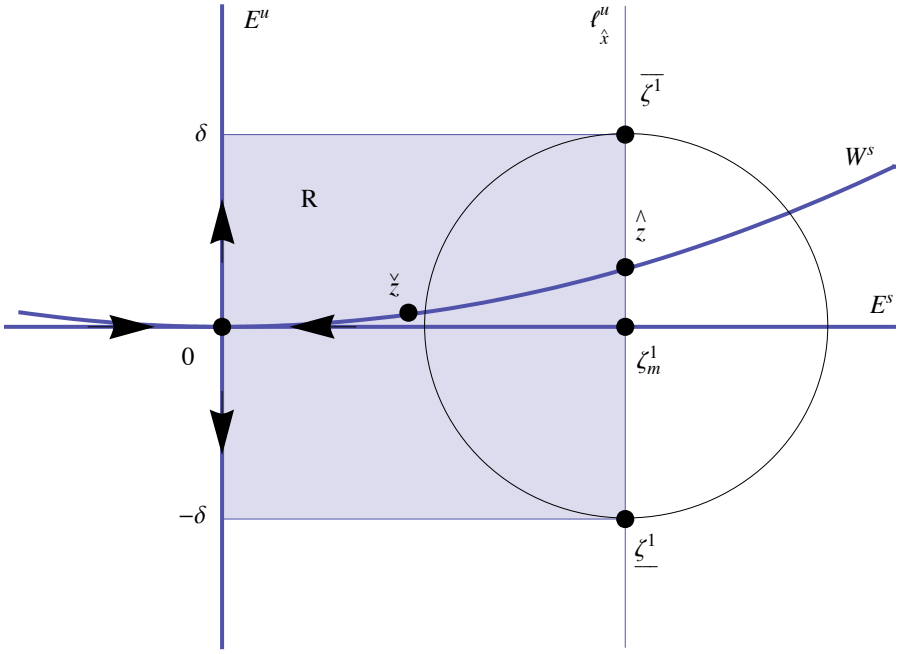

Figure 4.1: *Illustration of the algorithm for computing the local stable manifold.*

Recall the notation $B_r(\tilde{z}) = \{z \in \mathbb{R}^2 : ||z - \tilde{z}|| < r\}$ for a ball with radius r around the point $\tilde{z}$. The algorithm takes as input a point $\hat{x} \in \mathscr{X}$ near the origin, that is $|\hat{x}| < \varepsilon_0$ with $\varepsilon_0 \ll 1$, the rectangle R, and a given tolerance ε. It then determines an approximation $\hat{w}$ of $w\big(\hat{x}\big)$. Let $\zeta^1_m = (\hat{x}, 0)$ and $\hat{z} = \big(\hat{x}, w(\hat{x})\big)$. If $\delta > 0$ is sufficiently large then $\hat{z} \in B_\delta(\zeta^1_m)$. The ball $B_\delta(\zeta^1_m)$ intersects the line $x = \hat{x}$ in two points, namely $\overline{\zeta^1} = (\hat{x}, b_1)$ and $\underline{\zeta^1} = (\hat{x}, a_1)$, where $a_1 < b_1$. This situation is illustrated in Figure 4.1.

The algorithm uses the standard bisection method. Fix a time horizon

$$T_0 > \frac{\log\left(\delta/\varepsilon\right)}{\log \lambda^u}. \tag{4.4}$$

The point $\zeta^1_m = (\hat{x}, c_1) = (\hat{x}, 0)$ is the midpoint of the line segment $\underline{\zeta^1}\overline{\zeta^1}$. Let $\tau > 0$ be the smallest integer such that $(x_\tau, y_\tau) = \varphi^\tau(\zeta^1_m) \notin R$. Compute the

iterates $(x_t, y_t) = \varphi^t(\zeta_m^1)$ for $0 \le t \le T$, where $T = \min\{T_0, \tau\}$.

If $-\delta \le y_T \le \delta$ then $T = T_0$, $z_{T_0} \in R$ and $\hat{w} = c_1$, and the algorithm stops with

$$|\lambda^u|^{T_0}|\hat{w} - w(\hat{x})| \lesssim \delta$$

which implies, using (4.4), that

$$|\hat{w} - w(\hat{x})| \lesssim \varepsilon.$$

Otherwise, if $y_T > \delta$ then $c_1 > w(\hat{x})$; set therefore $a_2 = a_1$, and $b_2 = c_1$; if $y_T < -\delta$ set $b_2 = b_1$ and $a_2 = c_1$. Take $\zeta_m^2 = (\hat{x}, c_2)$ as the midpoint of the line segment $\underline{\zeta^2}\overline{\zeta^2}$, where $\underline{\zeta^2} = (\hat{x}, a_2)$ and $\overline{\zeta^2} = (\hat{x}, b_2)$. In this way sequences $\{\underline{\zeta^k}\}$ and $\{\overline{\zeta^k}\}$ are obtained such that $w(\hat{x}) \in [a_k, b_k]$. The algorithm stops if $|b_k - a_k| \le \varepsilon$, with output

$$\hat{w} = \frac{b_k - a_k}{2}.$$

Note that then $|\hat{w} - w(\hat{x})| \le \varepsilon/2$.

4.2.2 Computing the global stable manifold. To obtain a discretisation of the stable manifold W^s, set $\check{z} = \varphi(\hat{z})$ and $I_0 = [\check{x}, \hat{x}]$. An equidistant grid $\{x_0^1, ..., x_0^k\}$ on the interval $[\check{x}, \hat{x}]$ is introduced such that

$$\check{x} = x_0^1 < x_0^2 < .... < x_0^k = \hat{x}.$$

By the algorithm described above, approximations w_0^k to $w(x_0^k)$ are computed. Set $z_0^i = (x_0^i, w_0^i)$; the set

$$\mathscr{W}_0 = \left\{z_0^1, ..., z_0^k\right\}$$

is a discrete representation of the local stable manifold.

To obtain a discrete representation of the global manifold W^s the set $\mathscr{W}_0$ is iterated. Define

$$z_t^i = \varphi^t(z_0^i), \quad \text{where} \quad i = 1, ..., k \quad \text{and} \quad t = 1, 2, ..., N.$$

Then the set

$$\mathscr{W} = \left\{ z_0^1, z_0^2, ..., z_0^k, ..., z_N^{k-1}, z_N^k \right\} \tag{4.5}$$

is a discrete representation of W^s.

4.3 The value functions

Recall the two kinds of value functions introduced in Chapter 2: the orbit value function v (cf. equation (2.23)) and the value function $\bar{V}$ (cf. equation (2.24)).

In Section 2.2 it is shown that if the stable manifold of $\bar{z}$ can be represented as the graph of a function $y = w(x)$, then the local value function $\tilde{V}$ associated to $\bar{z}$ (cf. equation (2.22)) satisfies

$$d\tilde{V}/dx = w, \tag{4.6}$$

at least locally around $\bar{z}$. To recover the value function from w requires an integration. To find the values at other points in the state space the Bellman equation is used. It follows from equation (4.6) that

$$\tilde{V}(x) = \tilde{V}(0) + \int_0^x w(\xi)\, \mathrm{d}\xi.$$

As $w(0) = 0$, an approximation $\tilde{V}_{\approx}$ of $\tilde{V}$ is obtained by replacing w by its first order Taylor approximation

$$\tilde{V}_{\approx}(x) = \tilde{V}(0) + \int_0^x w'(0)\xi\, \mathrm{d}\xi. \tag{4.7}$$

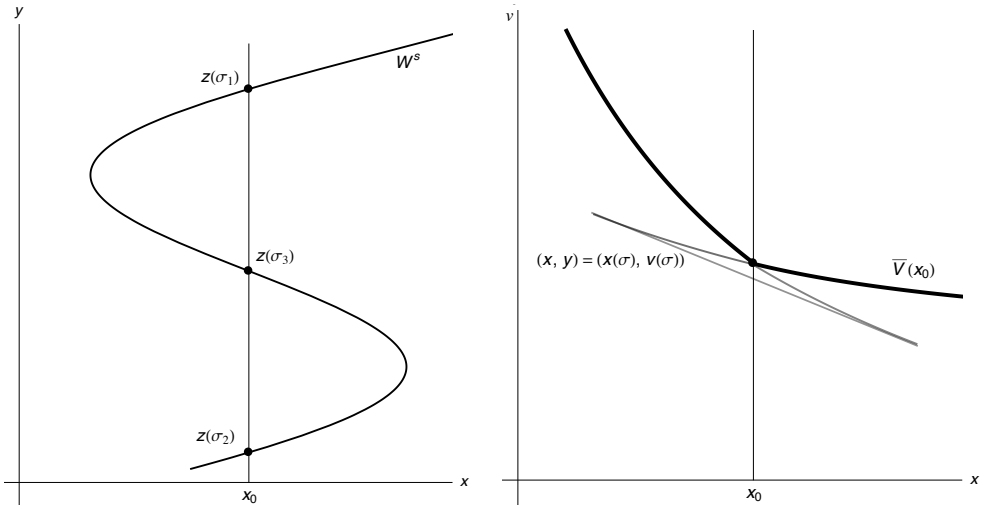

Figure 4.2: *The plot on the left shows a part of the stable manifold W^s parametrised by a parameter $\sigma \in \mathbb{R}$ as $z(\sigma) = (x(\sigma), y(\sigma))$. In the right hand plot, the orbit value function v, which associates the value $v(\sigma) = v(z(\sigma))$ to a point $z(\sigma) \in W^s$, is shown. The value function $\bar{V}$ associated to W^s is indicated by a black thick line. The state $x = x_0$ corresponds to an indifference point; at this state, the value function $\bar{V}$ has a kink.*

Note that $\left|\tilde{V}_{\approx}(x) - \tilde{V}(x)\right| \leq cx^3$, $c > 0$. A more accurate approximation could be achieved by a higher order approximation of the integral.

4.3.1 The value function and indifference points. In this section values for points of W^s are computed.

Suppose that $\mathbf{z} = \{z_t\}$ is an orbit starting at $z_0 \in W^s$. As seen in Chapter 2, the orbit value function $v(z_0)$ associated to W^s is defined as

$$v(z_0) = \tilde{J}(\mathbf{z}) = \sum_{t=1}^{\infty} G(z_{t-1})e^{-\rho t},$$

where G is given in (2.27). Note that it may happen that there are several

$z_0^{(1)}$, $z_0^{(2)}$, ... $\in W^s$ such that $x_0^{(i)} = x_0$. In this setting the definition of the value function $\bar{V}$ associated to W^s (cf. (2.24)) read as

$$\bar{V}(x_0) = \sup\left\{v(z_0^{(i)}) \,:\, x_0^{(i)} = x_0\right\}$$

(recall that $\sup\emptyset = -\infty$). The orbit value function v is approximated using the discrete representation $\mathscr{W}$ of W^s. For every point $z_t^l \in \mathscr{W}$ and for every $1 \leq l \leq k$ a value v_t^l is computed as follows. For $t = 0$, the approximation (4.7) is used to compute $v_0^l = \tilde{V}_{\approx}(x_0^l)$. For $t \geq 1$ the value v_t^l is computed using the Bellman equation

$$v_t^l = G(x_t^l, y_t^l) + e^{-\rho} v_{t-1}^l.$$

The set

$$\mathscr{V} = \left\{v_0^k, ..., v_N^{k-1}, v_N^k\right\}$$

is then a discrete representation of the orbit value function associated to W^s.

In order to obtain a discretisation of the value function $\bar{V}$ associated to W^s, an equidistant grid $\{x^1, x^2, ..., x^n\}$, $n > 0$, is introduced on $\mathscr{X}$. The elements of $\mathscr{W}$ are relabelled to obtain a sequence $\tilde{\mathbf{z}} = \{\tilde{z}_s\}_{s=1}^S$ in such a way that

$$\tilde{z}_{jk+i} = z_j^i, \quad 1 \leq i \leq k \quad \text{and} \quad 0 < j \leq N.$$

In the same way a sequence $\tilde{\mathbf{v}} = \{\tilde{v}_s\}_{s=1}^S$ of values is defined, such that $\tilde{v}_{jk+i} = v_j^i$.

Let $\pi : T^*\mathscr{X} \to \mathscr{X}$ be given as $\pi(x, y) = x$. A *turning point* of W^s is a point $z \in W^s$ such that $T_z W^s \subset \ker D\pi$, that is a point where W^s is tangent to the vertical direction. A *discrete turning point* is a point $\tilde{z}_s$ such that

$$(\tilde{x}_s - \tilde{x}_{s-1})(\tilde{x}_{s+1} - \tilde{x}_s) \leq 0.$$

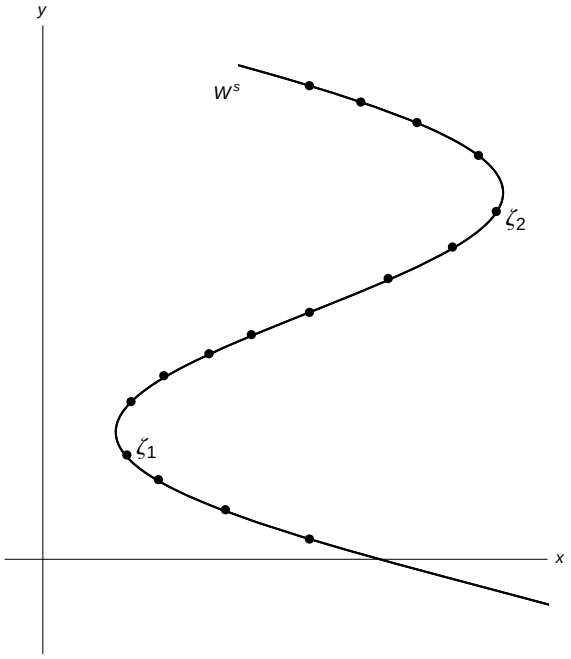

Figure 4.3: *Discrete turning points ζ_1 and ζ_2 of $\mathscr{W}$.*

Let $\zeta_1, \zeta_2, ..., \zeta_L$ be the sequence of discrete turning points of $\mathscr{W}$ (see Figure 4.3); that is $\zeta_i = \tilde{z}_{s_i}$ for $s_1 < s_2 < ... < s_L$. Introduce the notation

$$[a, b] = \{x | \min(a, b) \leq x \leq \max(a, b)\}.$$

If $x^n \in [\tilde{x}_i, \tilde{x}_{i+1}]$ then there is $\vartheta = \vartheta_i(x^n)$ such that $0 \leq \vartheta \leq 1$ and

$$x^n = (1 - \vartheta)\ \tilde{x}_i + \vartheta \tilde{x}_{i+1}.$$

Determine y^n and $\bar{v}^n$ by linear interpolation

$$\begin{aligned} y^n &= (1 - \vartheta)\tilde{y}_i + \vartheta \tilde{y}_{i+1}, \\ \bar{v}^n &= (1 - \vartheta)\tilde{v}_i + \vartheta \tilde{v}_{i+1}, \end{aligned}$$

where ϑ is as before. Note that x^n may be contained in several segments $S_\ell = \left[\zeta_\ell, \zeta_{\ell+1}\right]$. In this case, values for y^n_ℓ and $\bar{v}^n_\ell$ corresponding to each

segment are obtained. Let $\bar{v}_\ell^n = -\infty$ if $x^n \notin S_\ell$. Now $\bar{v}_\ell^n$ is defined for all $1 \leq \ell \leq L$.

The approximation of $\bar{V}(x^n)$ obtained is then given as

$$\bar{V}_{\approx}^n = \max_\ell \{\bar{v}_\ell^n\}.$$

If the maximum is obtained for $\ell = \ell^*$, then $(x^n, y_{\ell^*}^n)$ is an approximation to the initial point of the trajectory tending to $\bar{z}$ that has value $\bar{V}(x^n)$.

Finally indifference points are located numerically: these are states $x \in \mathscr{X}$ for which two different points $(x, y_1) = z_1 \in W^s$ and $(x, y_2) = z_2 \in W^s$ have both the same associated values $v(z_1) = v(z_2) = \bar{V}(x)$. A decision maker is indifferent between the trajectories starting at z_1 and z_2. To obtain an approximation to the indifference points, first the segment value function $V_\ell : \mathscr{X} \to \mathbb{R}$ corresponding to the segment S_ℓ is constructed. The V_ℓ's are piecewise linear functions, obtained by linear interpolation between points (x^n, V_ℓ^n) and (x^{n+1}, V_ℓ^{n+1}). A point $\hat{x}$ such that

$$V_{\ell_1}(\hat{x}) = V_{\ell_2}(\hat{x}) \quad \text{and} \quad V_{\ell_1}(\hat{x}) \geq V_\ell(\hat{x})$$

for all ℓ is a numerical approximation of an indifference point. A bisection method is used to find these points.

4.3.2 Indifference thresholds. Recall the assumption that the phase map φ has two saddle fixed points $z_- = (x_-, y_-)$ and $z_+ = (x_+, y_+)$, with $x_- < x_+$, and associated stable manifolds W_-^s and W_+^s. Let the value function corresponding to the stable manifold W_j^s be denoted by $\bar{V}_j$, $j \in \{-, +\}$.

Recall that an indifference threshold is an indifference point for which the originating optimal solutions converge to different steady states (see Chapter

3). To find an approximation of such a threshold the stable manifolds W^s_- and W^s_+ and their associated value functions $\bar{V}_-$ and $\bar{V}_+$ are computed by the methods which have been described in the previous sections. For a grid $\left(x^1, ..., x^n\right)$ in $\mathscr{X}$, piecewise linear functions $\bar{V}_j$, $j \in \{-, +\}$ are computed by linear interpolation between points $\left(x^n, \bar{V}_j(x^n)\right)$ and $\left(x^{n+1}, \bar{V}_j(x^{n+1})\right)$. Intersection points $(\breve{x}, \breve{y})$ of the graphs of these functions are then computed by the bisection method. The state component $\breve{x}$ of this point is a numerical approximation of the indifference threshold.

4.4 Determining indifference-attractor bifurcations numerically

This section deals with the numerical analysis of the indifference-attractor bifurcation curves. Consider the parametrised family $\varphi = \varphi_\mu$ of phase maps associated to the optimisation problem (4.1).

Indifference thresholds can be generated in an indifference-attractor bifurcation (see Chapter 3). In such a bifurcation, a semi-stable optimal state emerges as a parameter is varied and splits into a locally stable attractor and an indifference threshold. More precisely, there is a parameter value μ_c such that for $\mu < \mu_c$, the point x_+ is a global attractor for the optimal dynamics. For $\mu > \mu_c$, there is an indifference threshold x_s, and both x_- and x_+ are local attractors of the optimal dynamics. If $\mu = \mu_c$, then the orbit $x = x_-$ is semistable: all orbits starting to the left of it converge to x_-, while all orbits starting to the right converge to x_+. The bifurcation value μ_c is determined by a geometric criterion which is recalled next and which is used to compute the indifference-attractor bifurcation curve numerically.

4.4.1 Determination of the bifurcation parameter value. Assume that the parts of W^u_- and W^s_+ that interact in the heteroclinic bifurcation are parametrised by arclength, starting from the respective fixed points. That is, the parametrisations $\gamma_s(\sigma) = \big(x_s(\sigma), y_s(\sigma)\big)$ and $\gamma_u(\sigma) = \big(x_u(\sigma), y_u(\sigma)\big)$ satisfy $\gamma_u(0) = z_-$ and $\gamma_s(0) = z_+$, and $||\gamma_s'(\sigma)|| = ||\gamma_u'(\sigma)|| = 1$. Note that these parametrisations determine the orientations of W^s_+ and W^u_-. Using these parametrisations, the intersection number of a heteroclinic point $p = \gamma_s(\sigma_1) = \gamma_u(\sigma_2)$ is defined as $\mathrm{sgn}\Big(\det\big(\gamma_s'(\sigma_1)\gamma_u'(\sigma_2)\big)\Big)$, where

$$\mathrm{sgn}(x) = \begin{cases} 1 & \text{if } x > 0, \\ 0 & \text{if } x = 0, \\ -1 & \text{if } x < 0 \end{cases} \tag{4.8}$$

A heteroclinic orbit is upward if the intersection number of one point (and hence all points) of the orbit is $+1$ (cf. Section 3.3). Let $\mathbf{p} = \{p_t\}_{t=-\infty}^{\infty}$ be an upward heteroclinic orbit including W^s_+ and W^u_-. For simplicity assume that $\mathbf{p}$ is the only upward orbit. Moreover, assume that p_0 is such that smooth curves c^u, c^s as postulated in Assumption 3.1.6 exist, connecting p_0 to p_{-1}. The closed curve $c = c^s + c^u$ is then the boundary of a region A; the positively and negatively oriented components of A are defined by A^+ and A^- respectively (see Figure 4.4). The designation A_μ is used for A to stress the dependence on the parameter μ. As the family φ_μ goes through a heteroclinic bifurcation scenario, there is a parameter interval $[\mu_1, \mu_2] \subset \mathscr{P}$ such that for $\mu < \mu_1$ and $\mu > \mu_2$, the manifolds W^u_- and W^s_+ have no points in common, and for $\mu \in [\mu_1, \mu_2]$ there is at least one heteroclinic orbit. Moreover all heteroclinic orbits are necessarily tangencies at $\mu = \mu_1$ and $\mu = \mu_2$.

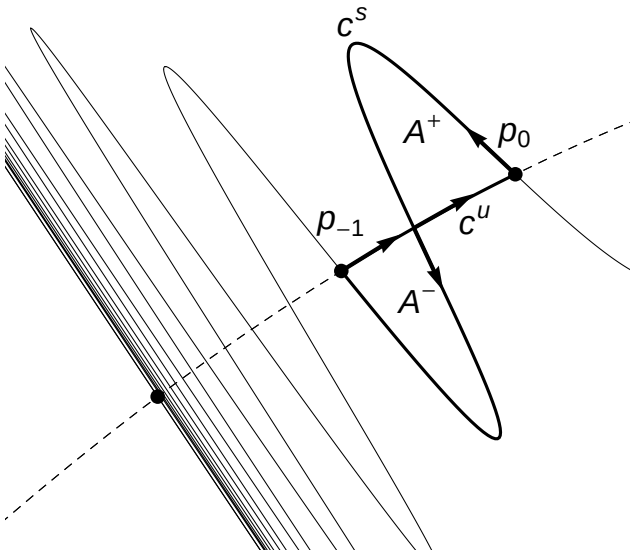

Figure 4.4: *The region A, bounded by the curve* $c = c^s + c^u$

Let

$$\Delta : (\mu_1, \mu_2) \to \mathbb{R}$$

be the function that assigns to each parameter $\mu_1 < \mu < \mu_2$ the area difference between A_μ^- and A_μ^+, that is

$$\Delta(\mu) = \Omega(A_\mu) = \text{ area}\,(A_\mu^-) - \text{ area}\,(A_\mu^+),$$

where Ω is as equation (3.4). Recall from Theorem 3.2.3 that at the indifference-attractor bifurcation

$$\text{area}\,(A_\mu^+) = \text{ area}\,(A_\mu^-);$$

that is, the bifurcation parameter value μ_c is a zero of $\Delta(\mu)$. Therefore, determination of μ_c amounts to solving the equation $\Delta(\mu) = 0$.

Let c_1^s and c_1^u be the segments of c^s and c^u which connects p_0 to r; similarly

c_2^s and c_2^u be the segments of c^s and c^u which connects r to p_{-1} respectively. The curves $c_1 = c_1^s + c_1^u$ and $c_2 = c_2^s + c_2^u$, which are the boundaries of the regions A^+, A^- receptively, are simple closed curves. Therefore given the orientation of A^+ and A^-, the areas of these regions are obtained as follows

$$\begin{aligned}\text{area}(A^+) &= \iint_{A^+} \mathrm{d}x\ \mathrm{d}y = \int_{c_1^u} y\ \mathrm{d}x - \int_{c_1^s} y\ \mathrm{d}x,\\ \text{area}(A^-) &= \iint_{A^-} \mathrm{d}x\ \mathrm{d}y = \int_{c_2^s} y\ \mathrm{d}x - \int_{c_2^u} y\ \mathrm{d}x.\end{aligned}$$

Hence

$$\Delta(\mu) \quad = \quad \text{area}(A^+) - \text{area}(A^-) = \int_{c^u} y\ \mathrm{d}x - \int_{c^s} y\ \mathrm{d}x.$$

Note that this formula is general, i.e. it does not depend on the assumption of $\mathbf{p}$ being the only upward orbit. If there are several upward orbits $\mathbf{p}^{(k)}$, $k = 1, 2, ..., K$, with $\mathbf{p}^{(1)} = \mathbf{p}$ then differences $\Delta^{(k)}(\mu)$ have to be computed for each of them. The indifference-attractor bifurcation then satisfies $\Delta^{(1)}(\mu_c) = 0$ and $\Delta^{(k)}(\mu_c) > 0$ for $k > 1$ (cf. Theorem 3.2.3).

Recall the parametrisation of W_+^s and W_-^u. There exist σ_i and $\bar{\sigma}_i$, $i = 1, 2$, such that $p_0 = \gamma_s(\sigma_1) = \gamma_u(\sigma_2)$ and $p_{-1} = \gamma_s(\bar{\sigma}_1) = \gamma_u(\bar{\sigma}_2)$. The line integrals in the expression of $\Delta(\mu)$ are rewritten as follows

$$\Delta(\mu) = \int_{\bar{\sigma}_2}^{\sigma_2} y_u(\sigma)\ x_u'(\sigma)\ \mathrm{d}\sigma - \int_{\sigma_1}^{\bar{\sigma}_1} y_s(\sigma)\ x_s'(\sigma)\ \mathrm{d}\sigma. \tag{4.9}$$

In this way a numerical approximation of Δ is obtained using the discrete representation of invariant manifolds computed in the previous section. The secant root finding method (see Atkinson (1989)) is used to solve the equation $\Delta(\mu) = 0$ and to obtain an approximation of the indifference-attractor bifurcation parameter value μ_c.

4.4.2 Bifurcation diagram in parameter space. In the previous section it was assumed that the the phase map φ depends on a scalar parameter μ. However, in applications the phase map may depend on vector-valued parameters. The method generalises easily to this more complex case, yielding bifurcation manifolds instead of bifurcation points.

In the special case that $\mathscr{P} \subset \mathbb{R}^2$ the equation $\Delta(\mu) = 0$ determines a curve in the parameter space, which can be computed by a continuation method.